

# APPLICATION OF AUTOMATIC CELL TRACKING FOR WOUND HEALING ASSAY IN VITRO

Ryoma Bise, Takeo Kanade, Zhaozheng Yin, and Seung-il Huh

Carnegie Mellon University, Pittsburgh, PA, USA.

## ABSTRACT

The wound healing assay *in vitro* is widely used for research and discovery in biology and medicine. This assay allows for observing the healing process *in vitro* in which the cells on the edges of the artificial wound migrate toward the wound area. The influence of different culture conditions can be measured by observing the change in the size of the wound area. For further investigation, more detailed measurements of the cell behaviors are required. In this paper, we present an application of automatic cell tracking in phase-contrast microscopy images to wound healing assay. The cell behaviors under three different culture conditions have been analyzed. Our cell tracking system can track individual cells during the healing process and provide detailed spatio-temporal measurements of cell behaviors including cell density, cell migration speed and direction, and the statistics of cell mitosis events. The application demonstrates the effectiveness of automatic cell tracking for quantitative and detailed analysis of the cell behaviors in wound healing assay *in vitro*.

**Index Terms**— Cell Tracking, Wound Healing Assay

## 1. INTRODUCTION

We present an application of automatic cell tracking for wound healing assay *in vitro*. The wound healing assay is an easy and low-cost method to allow for observing cell migration *in vitro* [1]. In this assay, cells are firstly grown to form a confluent monolayer *in vitro*. An artificial wound is generated by scratching and displacing a group of cells at the center as shown in Fig.1, and then the healing process is observed while neighboring cells fill in the wound area as shown in Fig.2 (a-c). This healing process takes 3 to 24 hours, depending on cell types and culture conditions. The healing process is monitored by a sequence of microscopic images.

The wound healing assay has been widely used in tissue culture to monitor cell behaviors under various culture conditions. Liang *et al.* [1] compared several migration assays *in vitro* and described advantages of using the wound healing assay that mimics cell migration *in vivo*. For example, endothelial cells (ECs) *in vitro* mimic the process in which ECs in the blood vessels migrate into the denuded area to close

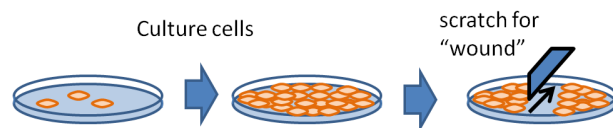


Fig. 1. The process of making wound.

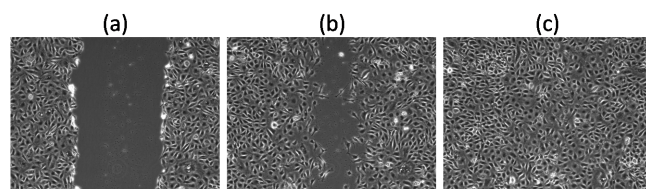


Fig. 2. Example images of the wound healing process. (a) the initial image on the healing process. (b) an image at which cells move to wound area. (c) an image at which cells fill the wound area.

the wound. Yarrow *et al.* [2] measured the healing speed by observing the size of the wound area in order to analyze the effectiveness of different culture conditions. For further analysis of the effectiveness of the cell culture conditions, more detailed measurements of the cell behaviors are often required. For example, Abbi *et al.* [3] analyzed the cell migration path to assess the effects of expression of exogenous genes on migration of individual cells. Nikolic *et al.* [4] manually tracked cell migration in wound healing assay in order to understand how multiple cells execute highly dynamic and coordinated movements during the healing process. Cell tracking allowed them to analyze how individual aspects of the wound contribute to the coordinated dynamics of cells. Zahm *et al.* [5] used a computer-assisted technique to quantitatively study the cell proliferation and migration during the wound healing process. Citing the difficulty of tracking cells in phase-contrast microscopy images, they used chemical compounds to create fluorescent images to track cells and count proliferative cells. Such chemical compounds generally interfere with the efficacy of drug candidates. Bunyak *et al.* [6] developed a cell tracking method for phase-contrast microscopy images and computed the time transition of the cell migration measures for 46 frames of a wound healing sequence.

In this paper, we present the application of our automatic

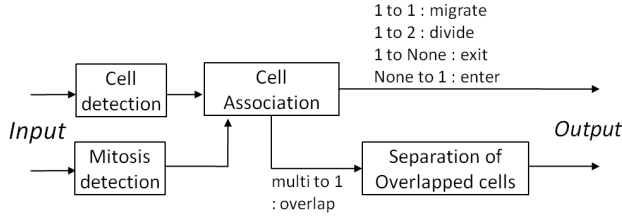


Fig. 3. Process of the cell tracking.

cell tracking method to long sequences of phase-contrast microscopy images of a wound healing assay *in vitro* in order to produce detailed quantitative analysis of the cell behaviors under three different culture conditions (i.e., three different amounts of medicine Latrunculin B that interferes with cellular activity). Our cell tracking system can track more than thousands of cells individually over long period under non-fluorescent imaging. It allows us to compute spatio-temporal measurements including the cell density, migration speed and direction, statistics of mitosis events, and their mutual dependency. These measurements can provide critical data for investigating the healing process.

## 2. AUTOMATIC CELL TRACKING METHOD

Fig. 3 shows the overview of our cell tracking system. Each image is processed in four steps: 1) *cell detection* detects and isolates blobs that can be individual cells or cell clusters (overlapping cells); 2) *mitosis event detection* locates mitosis events where and when one cell divides into two cells; 3) *cell association* performs data association between the cells in the previous frame and the blobs detected in the current frame as well as identifying cell clusters; 4) *separation of overlapping cells* decomposes each cell cluster to its member cells by using contour matching.

### 2.1. Cell Detection

Due to the interference optics of a phase contrast microscope, cells are surrounded by bright halos, and cellular fluid inside the membrane has similar intensity as the background. To facilitate segmentation, we have adopted the image restoration technique recently developed in [7]. The technique utilizes the optophysical principle of image formation by phase contrast microscope, and transforms an input image into an artifact-free images by minimizing a regularized quadratic cost function. In the restored image, cells appear as regions of positive values against a uniformly-zero background. A simple thresholding method, such as Otsu thresholding, can segment out the cell regions.

### 2.2. Cell Mitosis Event Detection

In the wound healing assay, it is important to locate individual cell birth event (time and location) at which one cell divides into two cells. To detect the birth events, we have adopted the mitosis detection technique recently developed in

[8]. Firstly, as mitosis events generally exhibits increase of brightness, bright regions are extracted as patches, and then candidate patch sequences are constructed by associating patches. Next, the gradient histogram features are extracted from the patches. Finally, a probabilistic model named Event Detection Conditional Random Field (EDCRF) is applied to determine whether each candidate contains a birth event and which frame the birth event is located in.

### 2.3. Cell Tracking

Based on the outputs of cell segmentation and mitotic event detection algorithms, we developed a cell-blob association algorithm performing data association between the cells in the previous frame and the blobs segmented in the current frame. The cell association algorithm makes the following hypotheses of all possible cell action and computes the likeliness of each hypothesis.

- (1) one-to-one: a cell migrates to a new position;

If the distance between the cell  $c_i$  in the previous frame and the blob  $b_j$  in the current frame,  $c_i \rightarrow b_j$  is a candidate of the migration hypothesis.

$$P_{1 \rightarrow 1}(c_i, b_j) = e^{-\frac{\|f(c_i) - f(b_j)\|}{\sigma}}$$

- (2) one-to-none: a cell exits from the field of view;

If the distance between the centroid of the cell at previous frame and the boundary of the field of view, the cell is a candidate of exit cells.

$$P_{1 \rightarrow 0}(c_i) = e^{-\frac{d(c_i)}{\lambda}}$$

- (3) none-to-one: a cell enters to the field of view;

If the distance between the centroid of the blob at current frame and the boundary of the field of view, the cell is a candidate of enter cells.

$$P_{0 \rightarrow 1}(b_i) = e^{-\frac{d(b_i)}{\lambda}}$$

- (4) one-to-two: a cell divide into two cells;

If a cell  $c_i$  is near a birth event detected by mitosis detection module, the cell is a candidate of a parent cell, and if combination of blobs  $b_{j_1}, b_{j_2}$  are near the candidate of parent cells, these blobs are candidates of the children cells.

$$P_{1 \rightarrow 2}(c_i, b_{j_1}, b_{j_2}) = e^{-\frac{\|f(c_i) - f(b_{j_1}, b_{j_2})\|}{\sigma}}$$

- (5) many-to-one: multiple cells overlap;

If several cells are close to each other in the previous frame and a nearby large blob is detected in the current frame, those cells have a many-to-one hypothesis

$$P_{n \rightarrow 1}(c_{i_1}, \dots, c_{i_n}, b_j) = e^{-\frac{\|f(c_{i_1}, \dots, c_{i_n}) - f(b_j)\|}{\sigma}}$$

where  $c_i$  represents the  $i$ th cell and,  $b_j$  represents the  $j$ th blob.  $f(\cdot)$  computes an object's feature vector where different types of features can be incorporated such as appearance histogram, shape and motion history. And  $d(c_i)$  is the distance between the centroid of cell  $c_i$  and the image boundary.  $\sigma$  and  $\lambda$  are free parameters to adjust the distribution. For more details of these hypotheses and formulations, we refer to [10].

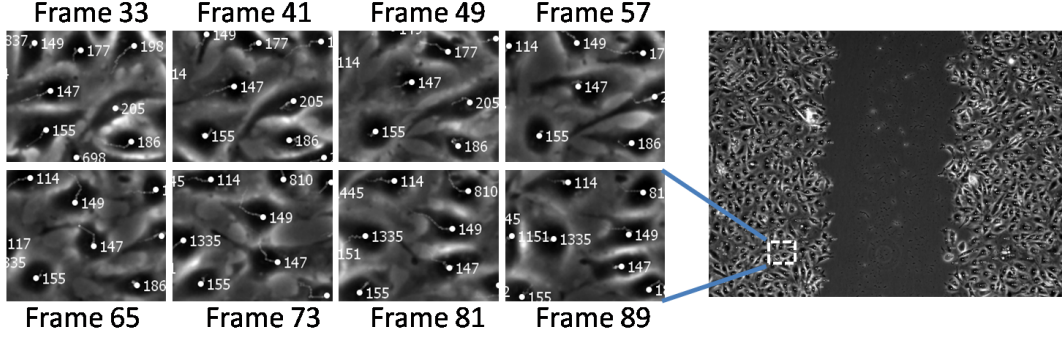


**Fig. 4.** Right: an example image of the tracking result. Left: an example image sequence of the zooming images that correspond with the white dot rectangle in the right image.

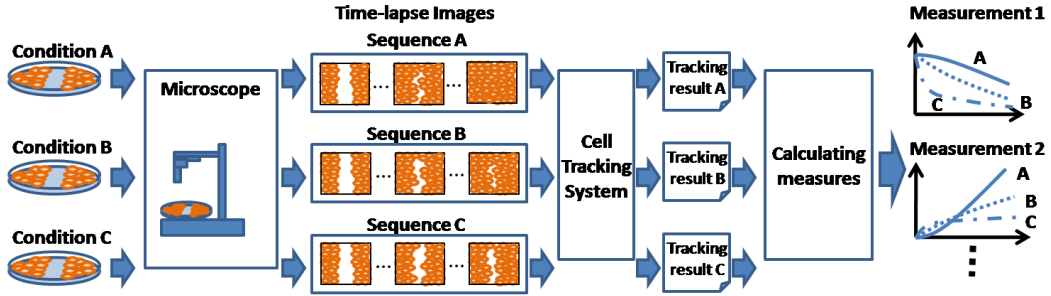


**Fig. 5.** Flow of our wound healing assay experiments under three culture conditions.

	control	10nM	100nM	average
Li et al. [9]	0.71	0.73	0.74	0.73
Ours	0.83	0.92	0.76	0.84

**Table 1.** Comparison of our system with [9].

The optimal association from the hypothesis set is found by solving an integer optimization problem which is similar to an optimization approach was used by [9] for track linking. When the system identifies a cell cluster (multi-to-one association), we apply a contour-matching method [11] to separate it into its member cells, thus the cell identities are maintained. Fig.4 shows an example of the tracking result where the cells are well tracked in high confluence.

#### 2.4. Performance Evaluation

The open area (wound area) is observed by a phase contrast microscope under three different cell culture conditions (we explain the conditions on the next section). The images are captured every 5 minutes and each sequence consists of 200 images with the resolution of 1392\*1040 pixels. To make groundtruth, we randomly pick forty cells at the beginning of each sequence and annotate the forty cells family trees through the 200th image. The total number of annotated cells in the three sequences is 27991.

We use a target effectiveness [12] to assess the system performance. The target effectiveness is defined as the number of target observations (human annoated) matched to the

best track (computer-generated) over the total number of target observations. It indicates how well targets are followed by tracks. As shown in Table 1, our system achieves higher target effectiveness than the state-of-the-art method in [9] on the sequences.

### 3. SPACE-TIME ANALYSIS OF CELL BEHAVIORS OF WOUND HEALING

We demonstrate how our automatic cell tracking can help to analyze the cell behaviors. Fig. 5 shows the overall flow of our wound healing analysis experiment. Firstly, the culture dishes with wound area are prepared under three culture conditions. These dishes are observed by microscope, generating a time-lapse image sequence. The image sequences are inputted to the automatic cell tracking system. From the tracking results, various measurements that characterize the cell behavior are calculated.

#### 3.1. Cell Culture Conditions

On three dishes, BAEC(bovine aortic endothelial cells) were cultured under three different culture conditions. For each dish, a group of cells at the center of the dish was scratched and displaced on a confluent monolayer. Different amount of medicine was added to each dish.

Condition A : control (no medicine)

Condition B : 10nM (nano molar) of Latrunculin B

Condition C : 100nM of (nano molar) Latrunculin B

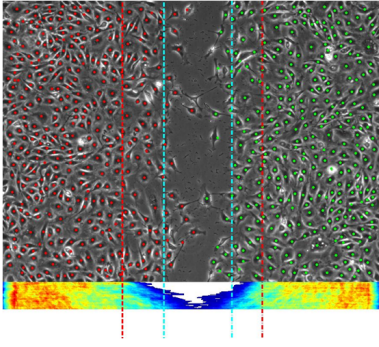


**Fig. 6.** The jet map of cell density changes over time with tracking results, each row of which represents the density. In the jet map, red color shows higher density, blue color shows lower density.

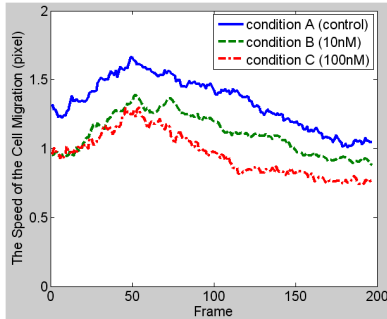


**Fig. 8.** The average speed of the cell migration over the time.

### 3.2. Cell Behavior Characteristic Measurements

Using tracking results, we calculated various measurements of cell behavior characteristics. In cell behavior analysis, the change of the cell density over time on the whole area is a useful index [13][14]. To investigate how the cell culture conditions affect the cell migration, speed and direction of the cell migration are often measured [13][15]. Cell culture condition usually affects both migration and proliferation. To separate these affects, the statistics of the mitotic events are important. Our system allows us to compute all of these spatio-temporal behavior characteristics in detail, including cell density, the speed and the direction of cell migration, and the statistics of mitosis events.

#### 3.2.1. Cell Density

Fig. 6 and 7 show how the cell density changes over time and location. Since cells generally migrate horizontally in the experiments as shown in Fig.2, the cell density is computed over narrow vertical window (the width of the window is 40 pixels, i.e.,  $36.5 \mu m$ ) as shown in Fig. 7(a). The vertical lines show that the 95% cell migration front of left and right

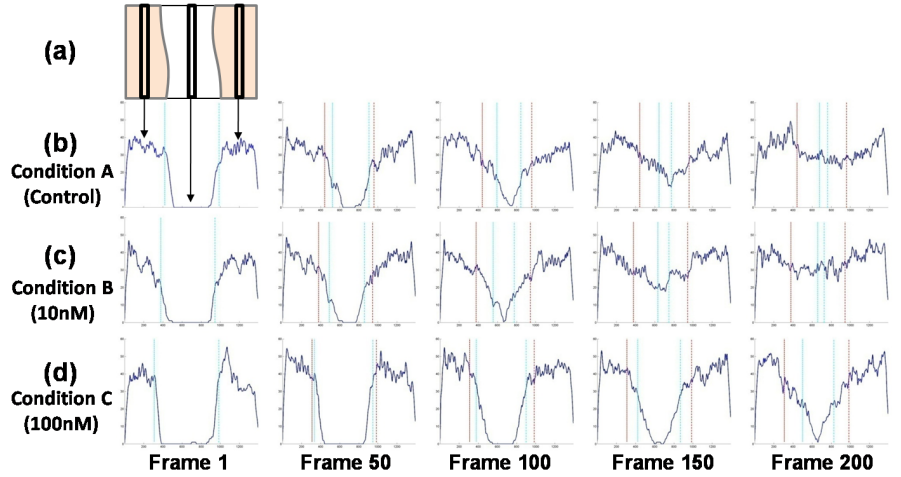


**Fig. 7.** The space-time transition of the cell density.

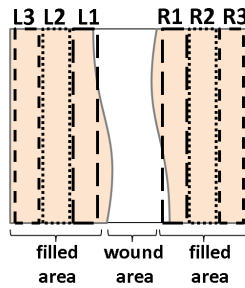


**Fig. 9.** Local areas.

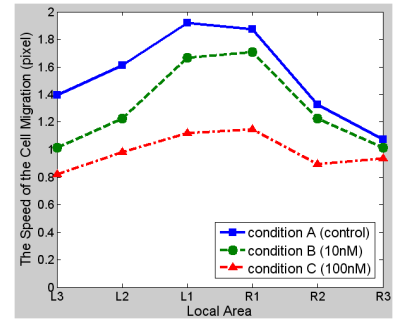


**Fig. 10.** The average speed of the cell migration at each local area.

sides, which is defined as the 95th percentile line of the total cell count of each side. Red color lines indicate the 95% line at the initial frame, blue dotted lines indicate the 95% line at the current frame. Fig. 7 (b-d) show the comparison of the space-time transition of the cell density under three different conditions. At the second row (condition A), the cell density in the wound area is low at frame 1. Then, cells in the left and right regions migrate into the central area and the density in the wound area increases until it becomes flat in frame 200. We observe the similar behaviors for the other conditions, but cells on condition C (100nM) migrate more slowly than those in condition A and B. The density in the wound area is still low at the end of the sequence.

#### 3.2.2. Speed of the Cell Migration

To analyze how the speed of cell migration changes over time, we computed the average speed of the cell migration over the whole area in each frame. The results presented in Fig. 8 show that the speed in the condition A (control) is consistently higher than those in other conditions, and the speed in the condition C (100nM) is the slowest. The migration speed firstly increases until frame 50, and then it continuously de-

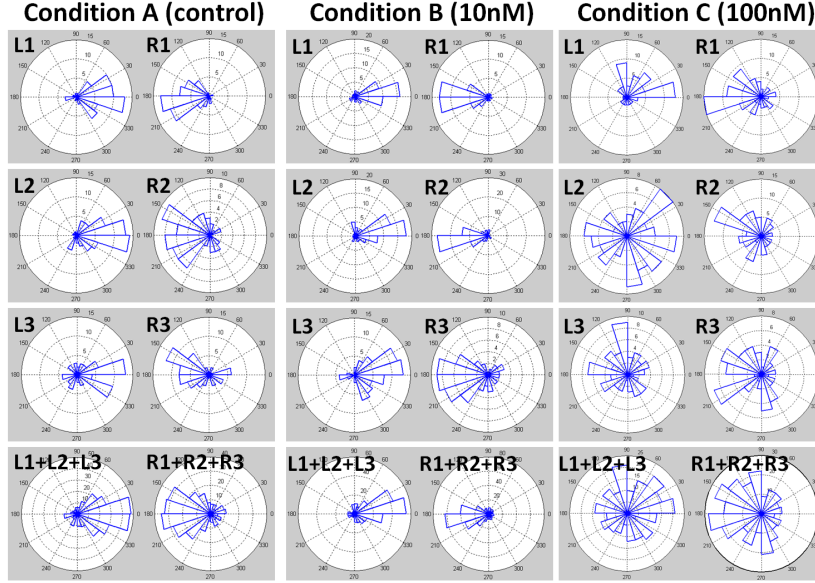


**Fig. 11.** Rose diagrams of cell migration directions on each local area.

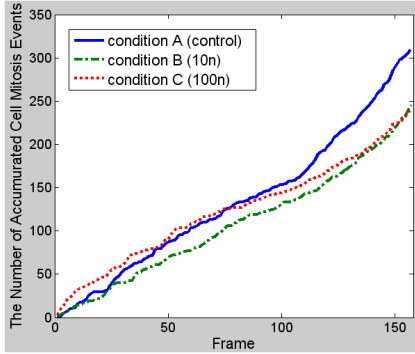


**Fig. 12.** The number of accumulated cell mitosis events at each frame.

crease with the time.

It is conceivable that the speed of the cell migration depends on the distance from the wound area. To know whether this is the case, the filled area (i.e., the left and right side of the wound area) is divided into six local areas as shown in Fig. 9. These local areas were defined based on the distance from the wound area, from L1 to L3 at the left side and from R1 to R3 at the right side away from the wound area. The cells on the edges of the wound area migrate toward the center, therefore, these local areas also move toward the center with the time. For each local area, the average speed of the cell migration is computed as shown in Fig. 10. Understandably, the cells in condition A (control) move faster than the others in every local area, and the cells in condition C (100nM) are the slowest. The graph indicates another interesting phenomenon in that the order of speeds are L1, L2 and L3 for the left side, and R1, R2 and R3 for the right side; that is, the speed of cell migration decreases with the distance from the wound edge.

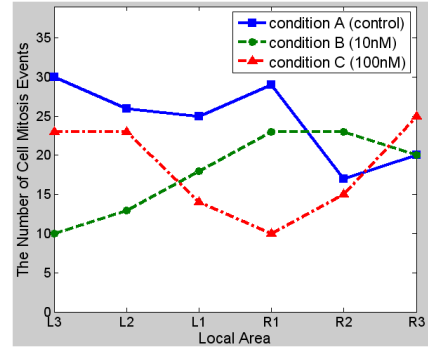


**Fig. 13.** The number of cell mitosis events at each local area.

### 3.2.3. Direction of the Cell Migration

To quantitatively analyze the direction of the cell migration, the distribution of cell migration directions on each condition was plotted by an angular histogram (rose diagram) as shown in Fig. 11. The first three rows show the distributions of the direction on each local area, respectively, for conditions A, B and C, and the bottom row shows the distributions on the whole areas left and right. We can observe that the cells tend to migrate toward the wound area in every local area on condition A and B. The cell migrations in L1, R1 (nearest area to the wound) are most highly directional to the direction to the wound. Also the graphs indicate an interesting phenomenon that cell migration in condition C (100nM) is less directed to the wound area ( $0^\circ$  for the left side,  $180^\circ$  for the right side). This means that the speed of the cell migration toward the wound area is the slowest in condition C (Fig. 6 (d)) not because the migration speed is slow, but because the migration direction is less directed.

### 3.2.4. Number of Cell Mitosis Events

To analyze how the number of cell mitosis events changes over time, we computed the number of accumulated mitosis events over the whole area. The results presented in Fig. 12 show that the number of mitosis events in the condition A (control) is higher than those in the other conditions. The curves of the accumulated number are almost linear. It indicates that the mitosis events occur consistently.

To show how the number of the cell mitosis events changes by location, the number of the cell mitosis events is computed over each local area as shown in Fig. 13. In this graph, we observe no distinctive characteristics. This means that the culture condition has more effects to the number of mitosis events than the distance from the wound area does.

## 4. DISCUSSION AND CONCLUSION

We presented the application of automatic cell tracking in phase-contrast microscopy images for wound healing assays *in vitro* in order to produce detailed quantitative analysis of the cell behaviors under three different culture conditions.

Understanding the cell behaviors is important to studying the influence of the environments including the types of medicines, the amount of the medicine, and materials in which these cells can grow. In the past, the simple measurement, such as the size of the wound area is often used, but such simple measures cannot provide the detailed analysis of cell behaviors. The spatio-temporal measurements of cell behaviors are important for critical analysis, because the cell culture conditions vary with time and space on the dish. Our system can provide such spatio-temporal cell behaviors measurements: the cell density, cell migration speed and direction, and statistics of cell mitosis events. The results of the experiments demonstrated the effectiveness of automatic cell tracking for quantitatively analyzing cell behaviors.

## 5. ACKNOWLEDGMENTS

We would like to thank cell tracking project members of Carnegie Mellon University: Dr. Sungeun Eom, Dr. Mei Chen, Elmer Ker, Dr. Phil Campbell and Dr. Lee Weiss. We really appreciate Dr. Naoki Yokoyama and Dr. Hideshi Hattori, who are working on Dai Nippon Printing, providing microscopy image sequences and a lot of comments about the cell behavior measurements to us.

## 6. REFERENCES

- [1] L. Chun-Chi, Y.P. Ann, and G. Jun-Lin, "In vitro scratch assay: a convenient and inexpensive method for analysis of cell migration in vitro," *Nature Protocols*, 2(2), 329-332, 2007.
- [2] C.J. MYarrow, E.Z. Perlman, J.N. Westwood, and J.T. Mitchison, "A high-throughput cell migration assay using scratch wound healing, a comparison of image-based readout methods," *BMC Biotechnology*, 4(21), 2004.
- [3] S. Abbi, H. Ueda, C. Zheng, A.L. Cooper, J. Zhao, R. Christopher, L.J. Guan, "Regulation of Focal Adhesion Kinase by a Novel Protein Inhibitor FIP200," *Molecular Biology of the Cell*, 13, 3178-3191, 2002.
- [4] L.D. Nikolic, N.A. Boettiger, D. Bar-Sagi, D.J. Carbeck, Y.S. Shvartsman, "Role of boundary conditions in an experimental model of epithelial wound healing," *Am J Physical Cell Physiol*, 291, 68-75, 2006.
- [5] J.M. Zahm, H. Kaplan, A.L. Herard, F. Doriot, D. Pierrot, P. Somelette and E. Puchelle, "Cell Migration and Proliferation During the In Vitro Wound Repair of the Respiratory Epithelium," *Cell Motility and the Cytoskeleton*, 37, 33-43, 1997.
- [6] F. Bunyai, K. Palaniappan, K.S. Nath, I.T. Baskin, and G. Dong, "Quantitative Cell Motility for in Vitro Wound Healing Using Level Set-Based Active Contour Tracking," *IEEE ISBI*, 1040-1043, 2006.
- [7] Z. Yin, K. Li, T. Kanade, and M. Chen, "Understanding the Optics to Aid Microscopy Image Segmentation," *MICCAI*, 2010.
- [8] S. Huh, E.D.F Ker, R. Bise, M. Chen, and T. Kanade, "Automated mitosis detection of stem cell populations in phase-contrast microscopy images," *IEEE Trans.Med. Imag*, In press.
- [9] K. Li, E.D. Miller, M. Chen, T. Kanade, L.E.Weiss, and P.G. Campbell, "Cell population tracking and lineage construction with spatiotemporal context," *Med Image Anal*, 12(5), 546-566, 2008.
- [10] T. Kanade, Z. Yin, R. Bise, S. Huh, S. Eom, M. Sandbothe, and M. Chen, "Cell Image Analysis: Algorithms, System and Applications," *IEEE Workshop on Applications of Computer Vision*, 2011, In press.
- [11] R. Bise, K. Li, S. Eom, and T. Kanade, "Reliably tracking partially overlapping neural stem cells in DIC microscopy image sequences," *MICCAI Workshop*, 2009.
- [12] S. Blackman, "Multiple-target tracking with radar applications," *Artech House Publishers*, 1986.
- [13] C.B. Isenberg, A.P. DiMilla, M. Walker, S. Kim, Y.J. Wong, "Vascular Smooth Muscle Cell Durotaxis Depends on Substrate Stiffness Gradient Strength," *Biophysical Journal*, 97, 1313-1322, 2009.
- [14] M. Tamura, J. Gu, K. Mtsumoto, S. Aota, R. Parsons, M.K. Yamada, "Inhibition of Cell Migration, Spreading, and Focal Adhesions by Tumor Suppressor PTEN," *Science*, 280, 1614-1617, 1998.
- [15] J. Gu, M. Tamura, R. Pankov, H.J. Erik, T. Takino, K. Mtsumoto, M.K. Yamada, "Shc and FAK Differentially Regulate Cell Motility and Directionality Modulated by PTEN," *Cell Biology*, 146, 390-403, 1999.